

THE PLANET AROUND 51 PEGASI¹

GEOFFREY W. MARCY,² R. PAUL BUTLER,² AND ERIC WILLIAMS

Department of Physics and Astronomy, San Francisco State University, San Francisco, CA 94132;
 gmarcy@etoile.berkeley.edu

LARS BILDSTEN²

Department of Physics, University of California, Berkeley, CA 94720

JAMES R. GRAHAM

Department of Astronomy, University of California, Berkeley, CA 94720

ANDREA M. GHEZ

Department of Astronomy, University of California, Los Angeles, CA 90024

AND

J. GARRETT JERNIGAN

Space Science Laboratory, University of California, Berkeley, CA 94720

Received 1996 September 19; accepted 1996 December 30

ABSTRACT

Doppler measurements of 51 Pegasi have been made from 1995 October through 1996 August, with a precision of 5 m s^{-1} . We find a period of 4.231 days, a velocity amplitude of $56 \pm 1 \text{ m s}^{-1}$, and a velocity curve that is essentially sinusoidal, all in excellent agreement with Mayor & Queloz. The only viable interpretation is a companion having minimum mass, $m \sin i = 0.45 M_{\text{Jupiter}}$, in a circular orbit of radius of 0.051 AU, with an eccentricity less than 0.01. Alternative explanations involving stellar surface phenomena such as pulsation or spots are ruled out. The lack of tidal spin-up of the star constrains the mass of the companion to be less than $15 M_{\text{Jupiter}}$. If the tidal Q -value is less than $\sim 10^6$ for the planet (close to Jupiter's presumed value), then internal dissipation is adequate to circularize the orbit and synchronize the planet's rotation. After subtracting the best-fit Keplerian velocity curve, the residuals exhibit no apparent variations at a level of 5 m s^{-1} during 10 months. The absence of further reflex motion along with limits from IR speckle observations rule out additional companions in a large portion of the parameter space of mass and orbital radius, including all masses greater than $1 M_{\text{Jupiter}}$ within 2.0 AU.

Subject headings: binaries: spectroscopic — planetary systems — stars: individual (51 Pegasi)

1. INTRODUCTION

Multiple Doppler measurements of the solar-type star 51 Peg reveal a velocity periodicity interpreted as due to a planetary companion (Mayor & Queloz 1995). The reported planet has an orbital radius of 0.05 AU, an orbital period of 4.229 days, and a minimum mass of $m \sin i = 0.46 M_{\text{Jupiter}}$ (hereafter M_J), where i is the unknown orbital inclination). The best-fit eccentricity is reported as $e = 0.09 \pm 0.06$, consistent with circular. No previous claim of a detected planetary companion to a main-sequence star has withstood scrutiny. If confirmed, the discovery of the first planet orbiting a solar-type star marks a watershed event in science.

The subsequent discovery of planetary companions around two other solar-type stars, namely, 47 UMa and 70 Vir (Marcy & Butler 1996; Butler & Marcy 1996), provided the first empirical sample of extremely low mass companions to solar-type stars. In retrospect, the companion to HD 114762 which exhibits $m \sin i = 10 M_J$ may represent the tip of the mass distribution of planetary companions or the lower end of the brown dwarf mass distribution (Latham et al. 1989; Mazeh, Latham, & Stefanik 1996). Recently, we

have identified three additional companions of planetary mass, namely, τ Bootis b, ρ^1 55 Cancri b, and ν Andromedae b (Butler et al. 1997; Baliunas et al. 1997). These three companions reside in orbits with periods less than 15 days, and have values of $m \sin i < 4 M_J$. Ongoing surveys at McDonald Observatory and at the Mount Hopkins Advanced Fiber Optic Echelle (AFOE) facility are likely to yield more planetary companions in the near future (Cochran & Hatzes 1994; Noyes et al. 1995).

Theoretical models of the interiors and evolutionary histories of extrasolar giant planets now provide clear predictions of their observable properties and evolutionary histories (Burrows et al. 1995; Saumon et al. 1996; Guillot et al. 1996; Burrows et al. 1996). However, the origin and homogeneity of the planetary companions remain in question (Lin, Bodenheimer, & Richardson 1996). It is not clear whether they formed by processes similar to those that lead to the planets in our solar system. Two of the extrasolar companions exhibit sizable orbital eccentricities, prompting some to classify them as “brown dwarfs.” Such objects are commonly defined to have masses less than $80 M_J$, which is required to sustain equilibrium hydrogen burning. However, the companions mentioned above all have $m \sin i$ less than $10 M_J$, far less than $80 M_J$. Indeed, only one bona fide brown dwarf companion is known (Nakajima et al. 1995). We shall use the term “planet” for the companions having $m \sin i < 10 M_J$, since it connotes objects having masses, diameters, orbital dimensions, and probably interior structures that are comparable to those of the giant planets in our solar system. The formation processes for

¹ Based on observations obtained at Lick Observatory, which is operated by the University of California, and on observations obtained at the W. M. Keck Observatory, which is operated jointly by the University of California and the California Institute of Technology.

² Also at Department of Astronomy, University of California, Berkeley, CA 94720.

both the new extrasolar planets and for planets in our solar system remain at the frontier of current theory.

2. OBSERVATIONS

A total of 110 spectra of 51 Peg have been obtained, spanning 300 days from 1995 October 11 through 1996 August 9. The spectra were obtained at Lick Observatory using the Hamilton echelle spectrograph (Vogt 1987). Both the 3 m Shane and the 0.6 m CAT telescopes were used to feed the Hamilton. An iodine absorption cell is used to impose wavelength markings directly on the spectrum, against which to measure stellar Doppler shifts. The iodine velocity technique has been described in detail (Butler et al. 1996b).

Doppler velocity errors are typically 5 m s^{-1} for observations with a signal-to-noise ratio (S/N) > 70 , and better for higher S/N . This is demonstrated in Figure 1, which shows the measured Doppler velocities for two stable stars with spectral types similar to that of 51 Peg. These observations cover the same interval of time over which the 51 Peg observations were made and exhibit a scatter of 5 m s^{-1} . No night-to-night or artificial corrections to the velocity zero point have been made.

The measured Doppler velocities of 51 Peg are listed in Table 1 and shown in Figure 2, exhibiting variations well in excess of the errors. A Keplerian velocity curve fits the data well, as shown by the solid line in Figure 2. The residuals to the fit (shown at the bottom of Fig. 2) have an rms scatter of 5.2 m s^{-1} , consistent with both the internal error of the individual measurements and the observed scatter of stable stars shown in Figure 1. Most of the observations shown in Figures 1 and 2 were obtained with the 0.6 m coude auxiliary telescope and typically have a S/N of only 70. The few observations made on the 3 m telescope usually have $S/N > 200$ and an internal error of 3 m s^{-1} .

A phased version of the 51 Peg velocities is shown in Figure 3. The underlying solid line is the same best Keplerian fit to the data. The phased plot shows that the phase, as well as period, of the velocity variations was maintained during the entire 10 month duration of observations. The best-fit orbital parameters are given in Table 2. The inferred orbital period is 4.2311 ± 0.0005 days, the velocity semiamplitude is $K = 55.9 \pm 0.8 \text{ m s}^{-1}$, and the eccentricity

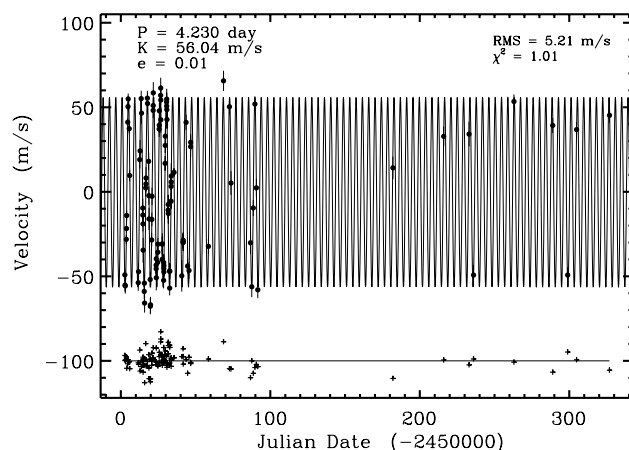


FIG. 2.—Doppler velocities for 51 Peg spanning 325 nights. A Keplerian orbital fit (solid line) is shown with a period of 4.231 days. The residuals to the orbital fit are shown at the bottom of the figure, exhibiting an rms of 5.2 m s^{-1} , consistent with expected errors. The residuals show no evidence of a second orbiting companion, at a threshold of 5 m s^{-1} .

is $e = 0.012 \pm 0.01$. The velocity variations are essentially sinusoidal, consistent with a circular orbit. Adopting a mass for the primary star of $1.0 M_{\odot}$ (see next paragraph), the orbital parameters imply a mass of $m \sin i = 0.445 \pm 0.01 M_J$ for the companion. All of the above orbital parameters agree with those of Mayor & Queloz (1995) within the errors. Our precision of 5 m s^{-1} and the numerous observations provide superior determinations of K and e , while the two sets of velocities give comparable quality in the period determination.

Table 3 gives measured properties of 51 Peg, many of which are reviewed by Henry et al. (1996). The recent parallax determination, $65.1 \pm 0.8 \text{ mas}$, from the *Hipparcos* satellite provides an excellent luminosity determination (Perryman et al. 1996). Photometry and spectroscopy lead to a self-consistent model of the star as a near solar twin of spectral type G2–3 V, slightly evolved off the main sequence, with weak chromospheric and coronal emission. Its rotation period is between 29.6 and 37 days, as determined from both the average level chromospheric Ca II H and K emission and the possible rotational modulation of

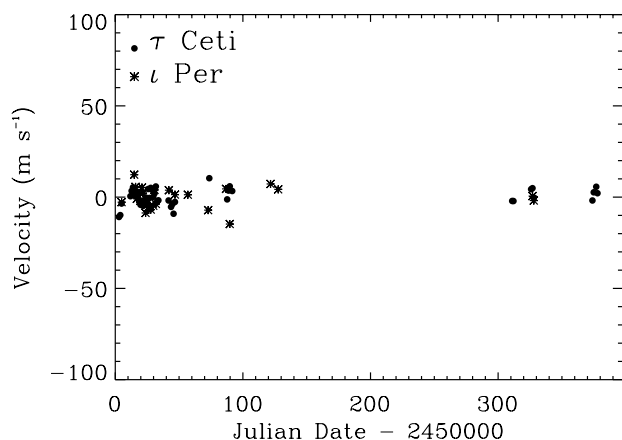


FIG. 1.—Doppler velocities of two stable reference stars. The rms scatter in the velocities of both τ Ceti and ι Per is 5 m s^{-1} . These observations were made over the same time span as those for 51 Peg, and illustrate the typical long-term errors of the Doppler measurements.

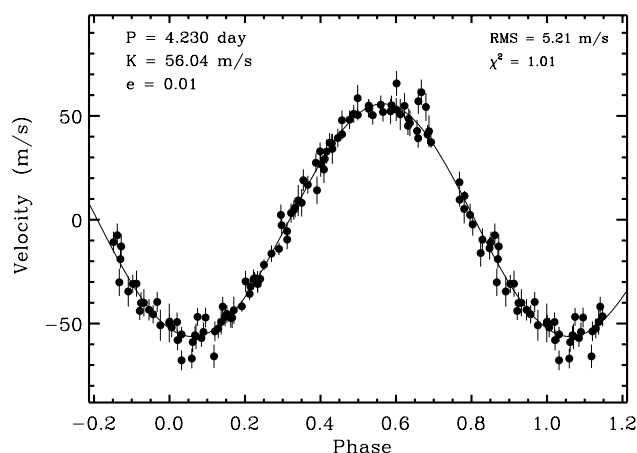


FIG. 3.—51 Peg velocities phased with the Keplerian fit. The variation is sinusoidal with a period of 4.231 ± 0.001 days. Phase stability is precisely maintained during 10 months.

TABLE 1
DOPPLER MEASUREMENTS FOR 51 PEG

JD - 2,450,000	Velocity (m s ⁻¹)	Error (m s ⁻¹)
2.67365	-40.87	3.3
2.80873	-46.96	3.6
2.95979	-47.39	4.5
3.62695	-19.85	2.9
3.73265	-13.47	2.6
3.90077	-5.782	3.0
4.60753	49.41	2.2
4.78429	58.66	2.5
4.90699	63.20	3.2
5.60503	45.60	2.7
5.92544	17.88	3.3
11.6443	-45.50	4.7
11.8378	-38.98	4.9
12.6355	27.27	5.2
12.8664	32.45	6.5
13.6242	63.38	4.6
13.8295	54.78	6.2
14.6428	-1.340	5.4
14.7229	-5.477	5.5
14.8161	-10.73	4.4
14.9043	-26.29	7.3
15.6261	-50.68	4.6
15.7467	-45.78	4.6
15.8654	-57.54	5.6
16.6149	10.56	5.0
16.7592	12.91	4.6
16.8474	16.40	6.6
17.7341	63.64	4.4
17.8442	60.48	6.0
18.6161	26.29	5.2
18.7648	5.988	5.4
18.8540	-7.798	6.5
19.6218	-43.62	4.7
19.7325	-59.45	4.8
19.8473	-58.60	4.7
20.6137	-20.22	4.0
20.7401	-8.064	4.0
20.8543	5.596	5.2
21.6151	56.41	4.5
21.6620	59.26	4.3
21.7063	66.78	6.4
23.5986	-35.13	5.1
23.6448	-37.30	4.4
23.6904	-31.35	4.9
23.7258	-42.57	7.5
24.6391	-33.47	2.6
24.7261	-27.46	3.0
24.8174	-22.70	3.7
25.6226	45.34	4.6
25.7145	47.61	4.5
25.7615	56.15	4.7
26.6176	65.32	6.1
26.6508	69.63	6.1
26.7020	62.54	6.7
26.7366	50.86	7.7
27.6474	-22.66	4.3
27.6893	-22.55	6.3
27.7399	-31.82	5.2
27.7721	-31.72	6.5
28.6061	-44.12	4.7
28.6556	-33.59	4.8
28.7019	-37.10	4.8
28.7450	-39.13	4.6
28.7799	-35.32	6.6
29.6093	25.09	4.3
29.7001	35.69	4.5
29.7468	41.17	4.3
30.6004	61.33	5.6
30.6454	58.98	7.5
30.6930	63.07	6.1
30.7402	56.86	5.0
30.8334	50.98	5.3

TABLE 1—Continued

JD - 2,450,000	Velocity (m s ⁻¹)	Error (m s ⁻¹)
31.6619	-2.545	5.0
31.7052	0.7633	5.7
31.7492	-4.599	5.9
32.6045	-38.53	4.3
32.6479	-48.68	4.3
32.6943	-38.84	4.7
33.6073	2.696	4.4
33.6527	11.46	4.6
33.6982	14.02	4.6
33.7331	17.55	7.5
35.5970	19.74	2.4
40.7493	-41.45	9.3
41.6045	-21.47	5.1
41.6932	-20.37	4.7
41.7388	-21.67	5.2
43.6442	49.31	4.6
44.6498	-35.66	4.4
45.6065	-38.28	4.8
46.6779	34.98	6.1
46.7230	37.54	4.9
58.5843	-24.00	4.4
68.6826	73.89	5.9
72.6462	58.57	4.5
73.6713	13.45	7.0
86.7296	-21.90	6.6
87.5888	-47.91	6.1
88.6111	-1.292	4.6
89.6847	60.15	4.6
90.6612	10.59	5.3
91.6137	-49.72	4.9
182.026	22.41	6.7
215.981	41.06	5.8
232.969	42.39	7.2
235.954	-40.99	6.0
262.991	61.66	4.2
288.933	47.51	4.5
298.923	-40.99	4.6
304.889	45.03	4.4
326.896	53.51	4.4

that emission (Noyes et al. 1984; Henry et al. 1996). Measured values of rotational $v \sin i$ span the range 1.7–3.0 km s⁻¹ (Soderblom 1983; Mayor & Queloz 1995; Valenti, Butler, & Marcy 1995; Hatzes, Cochran, & Johns-Krull 1996; François et al. 1996).

There is some concern about the internal consistency of the rotation period and $v \sin i$, as pointed out by Hatzes et al. (1996). The stellar radius must be between 1.1 and 1.3 R_{\odot} , as determined from the stellar luminosity and effective temperature or from the gravity. Adopting values of $R = 1.2 \pm 0.1 R_{\odot}$ and $P_{\text{ROT}} = 33 \pm 4$ days, one finds an equatorial velocity $V_{\text{eq}} = 1.8 \pm 0.4$ km s⁻¹, which is lower than all but one measured value of $v \sin i$. The highest resolution spectroscopy (Hatzes et al. 1996; François et al. 1996) suggests $v \sin i = 2.35$ km s⁻¹, which is slightly inconsistent with $V_{\text{eq}} = 1.8 \pm 0.4$ km s⁻¹. The uncertainties in R and P_{ROT} (which lead to the uncertainty of 0.4 km s⁻¹) are quite firm, which suggests that the actual value of $v \sin i$ is less than 2.2 km s⁻¹. Perhaps the measurements of $v \sin i$ have been overestimated slightly. Such errors could be caused by the slightly evolved status and enhanced metallicity of 51 Peg that could cause additional macroturbulent broadening beyond the reach of our current models. In any case, the large measured values of $v \sin i$ suggest that the star is viewed nearly equator-on. If the rotation and orbital

TABLE 2
ORBITAL PARAMETERS OF 51 PEG

Parameter	Mayor & Queloz	This Paper	Uncertainty
P (days)	4.2293	4.2311	0.0005
T_0^a (JD)	2,449,797.773	2,450,203.947	0.03
e	0.012	0.01
ω (deg)	Undefined	Undefined	...
K_1 (m s $^{-1}$)	59	55.9	0.8
$a_1 \sin i$ (m)	3.4×10^6	3.25×10^6	0.05×10^6
f_1 (m) (M_\odot)	9.1×10^{-11}	7.64×10^{-11}	...
N	35	110	...
rms $O - C$ (m s $^{-1}$)	13 ^b	5.2	...

^a Time of peak velocity.

^b After removal of long-term variations.

axes are nearly parallel, then the planet's mass is likely to be close to $0.45 M_J$, as $\sin i$ would be near unity.

3. ALTERNATIVE EXPLANATIONS

The measured Doppler shifts of the absorption lines of 51 Peg could, in principle, be explained by effects that involve only motions of the stellar surface, thereby eliminating need for an orbiting companion. Mayor & Queloz (1995) considered the possibilities of rotation of spots across the hemisphere and of stellar pulsation, and they provided evidence against both. These possibilities are now reconsidered in light of new photometry and high-resolution spectroscopy.

3.1. Spots and Photospheric Turbulence

Starspots could cause spurious Doppler shifts as they rotate across the visible stellar hemisphere and alternately occult the approaching and receding limbs. The resulting asymmetries of the shapes of the absorption lines would recur with a characteristic period equal to the rotation period of the star (with a fidelity depending on spot lifetime). The inferred rotational period of 33 ± 4 days is inconsistent with the 4.231 day Doppler periodicity. Thus, the possibility of spot-induced velocity variations seems ruled out. Such a prospect is also ruled out by the lack of photometric variability at a level less than a millimagnitude (Guinan 1995; Henry et al. 1996; Perryman et al. 1996). In addition, we have measured the intensities of the cores of all three Ca II infrared triplet lines which reflect chromospheric emission from the star. We find no significant variation in the core emission from our 100 spectra of 51 Peg, and a periodogram analysis reveals no peak near 4.2 days. Thus, there is no evidence for a chromospheric or magnetic origin

for the 4.2 day velocity period. We also find no significant periodogram peaks at any other period from 2 to 160 days, including the expected rotation period.

There remains an insidious possibility that the stellar surface is covered with a zebra-like spot or stripe pattern consisting of n spots periodically distributed over the 360° of longitude (Pettersen, Hawley, & Fisher 1992). An even number of equally distributed spots, $n = P_{\text{ROT}}/4.23$ days, would present nearly a constant apparent brightness. As one spot disappears beyond the receding limb, another emerges around the approaching limb. A total of eight such dark regions might suffice, having long-lived spatial integrity, perhaps due to an underlying magnetic origin. Such a scenario would still cause alternately covered limbs, thus producing periodic net Doppler shifts in the integrated flux spectra. This scenario is ruled out by the extreme constancy of the line profile shapes in 51 Peg observed by Hatzes et al. (1996). The velocity amplitude of 56 m s^{-1} implies that distortions of that extent would propagate through the line profiles with a period of 4.23 days, which is not seen in the Hatzes et al. spectroscopy.

3.2. Pulsation

The observed Doppler velocity variations of 51 Peg may be due to radial or nonradial pulsation. For radial pulsation, one may calculate the maximum change in radius by integrating the Doppler velocity curve over half a cycle. Assuming a standard projection factor of 1.3 (Carroll 1928; Butler, Bell, & Hindsley 1996a), the change in radius would be $0.01 R_\odot$, and the change in surface area would be 2%. The photospheric temperature was shown to be constant within 4 K during one cycle (Hatzes et al. 1996). Therefore, a

TABLE 3
51 PEG PROPERTIES

Parameter	Value	Source
T_{eff} (K)	5724–5755	Valenti et al. 1995; Edvardsson et al. 1993
M_V	4.56	Perryman et al. 1996 (<i>Hipparcos</i>)
L/L_\odot	1.24	From $M_V - M_V(\odot)$
Log gravity (cgs)	4.18–4.3	Edvardsson et al. 1993; Valenti et al. 1995
R/R_\odot	1.13–1.27	L , T_{eff} ; log g
Spectral type	G2–3 V	Houk 1995
R'_{HK}	–5.037	Noyes et al. 1984
P_{ROT} (days)	29–37	Baliunas et al. 1997; Henry et al. 1996
$V \sin i$ (km s $^{-1}$)	1.7–3	Hatzes et al. 1996
[Fe/H]	+0.06 to +0.192	Edvardsson et al. 1993; Valenti et al. 1995
Age (Gyr)	8.5	Edvardsson et al. 1993
Parallax (mas)	65.1 ± 0.8	Perryman et al. 1996

radius change would lead to brightness variations of 0.02 mag, which are clearly not observed, as discussed above. In addition, the period of 4.23 days is longer than the theoretically predicted radial pulsation period (Hatzes et al. 1996).

A search for nonradial pulsation in 51 Peg was first conducted by Mayor & Queloz (1995) by examining the bisector of the cross-correlation function. The bisector was found to be stable at the level of 2 m s^{-1} . A search for nonradial pulsation has also been conducted by Hatzes et al. (1996) by examining, at high spectral resolution, the shapes of the absorption-line profiles. No variation is seen at a level of 20 m s^{-1} , well below the Doppler variations of 56 m s^{-1} . This rules out nonradial modes for all l -values having $l = 4$ or greater. Values of $l = 1, 2, 3$ are still permitted as explanations. There is no obvious mechanism by which individual modes would be excited in an isolated G dwarf, while leaving other modes quiet.

4. ADDITIONAL COMPANIONS

The velocities of Mayor & Queloz (1995) indicate long-timescale variations in the velocity zero point of the 4.23 day sine wave of 51 Peg. The apparent “gamma velocity” of the sinusoid decreases by 20 m s^{-1} during the first 100 days of observation and then increases by 35 m s^{-1} during the subsequent 240 days. Mayor & Queloz (1995) interpret these “residual” velocities from the basic 4.23 day sinusoid as possibly caused by gravitational perturbations from a second companion. The residuals suggest an orbital period of 1.5–2.5 yr with a velocity semi-amplitude of $20\text{--}30 \text{ m s}^{-1}$. Duquennoy & Mayor (1991) give an upper limit to any velocity variations of 200 m s^{-1} during 12 yr.

Our Doppler measurements provide an opportunity to constrain the mass and period of any prospective companions. As shown in Figure 2, our velocity residuals to the Keplerian fit exhibit a scatter of only 5.2 m s^{-1} , consistent with the errors. So any actual “signal” in the residuals must have an amplitude below the scatter of 5.2 m s^{-1} during 300 days.

We model our sensitivity to additional companions by presuming them to be in circular orbits having a range of orbital periods and masses. We adopt an orbital phase such that the sinusoidal velocity variations reach maximum velocity at the midtime of our observational time series. This choice of phase produces the least detectable change in velocity, thereby yielding conservative mass thresholds. We deem “detectable” any companion that produces a maximum velocity variation that is at least twice the velocity errors, taken to be 5.2 m s^{-1} . Thus, we demand that the second companion induce velocity variations of at least 2σ during its most constant phase in order to be detected.

This 2σ detection criterion is illustrated in Figure 4, which shows the actual velocity residuals for 51 Peg superimposed on two hypothetical velocity curves for a companion of $m \sin i = 1 M_J$ having an orbital radius of either 1.3 or 1.7 AU. For an orbital radius of 1.3 AU, the orbital period is short enough that significant detectable variation would occur. Such a companion can be ruled out. For a larger orbital radius of 1.7 AU, the longer orbital period (and lower velocity amplitude) make the hypothetical velocity curve rise above residuals by only slightly more than 2σ , thus rendering this companion only marginally detectable. Companions having $m \sin i = 1 M_J$ but orbiting farther than 2 AU would not yet be detectable, owing to the short duration, 300 days, of measurements.

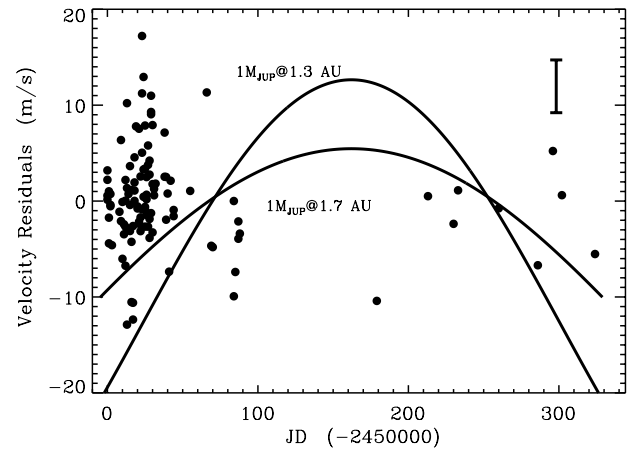


FIG. 4.—Hypothetical velocity curves (solid lines) due to additional companions, overplotted on the velocity residuals (filled circles). The upper solid line shows the Doppler velocity signal of a hypothetical planet having $m \sin i = 1 M_J$ orbiting at 1.3 AU. This variation is greater than the velocity residuals shown, ruling out such companions. The lower solid line shows the Doppler variations for a $1 M_J$ planet orbiting at 1.7 AU, which is only barely consistent with the velocity residuals.

A summary of this detectability criterion is shown in Figure 5, which shows the detectability for companion masses $m \sin i$ having possible orbital radii from 0 to 5 AU. At 1 AU, companions having $m \sin i$ greater than $0.2 M_J$ are just detectable. At 3 AU, companions must have $m \sin i$ greater than $7 M_J$ to be detectable. The second companion suggested by the velocities of Mayor & Queloz (1995) would have an orbital radius of 1.3–1.8 AU with a mass $m \sin i = 1 M_J$. Such a second companion seems unlikely, given the lack of variation of the residuals found here. The possibility remains that a second companion having $m \sin i \approx 1 M_J$ might exist farther than 2 AU from the primary. As our time baseline increases beyond the current 300 days, we will be able to detect additional companions beyond 2 AU.

5. INFRARED OBSERVATIONS

We have also carried out K-band speckle imaging observations at the W. M. Keck 10 m telescope located on

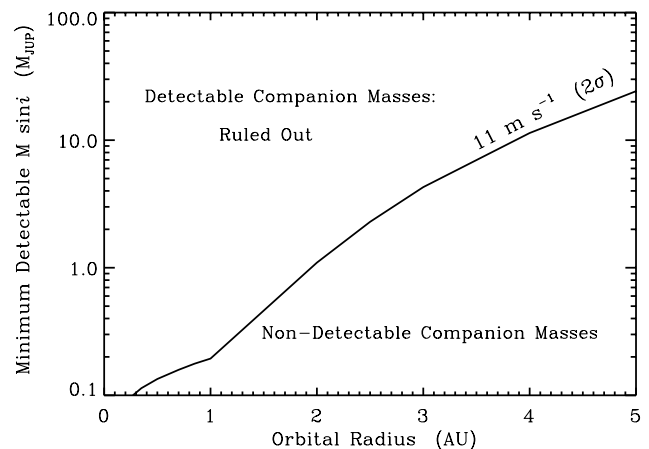


FIG. 5.—Detectability of an additional companion to 51 Peg, in parameter space of orbital radius and planetary mass, $m \sin i$. The solid line separates the high-mass detectable domain (upper) from the undetectable domain (lower). The upper domain represents additional companions to 51 Peg which can now be ruled out by the constancy of the velocity residuals to the Keplerian fit for the first companion. Companions more massive than $1 M_J$ within 2 AU are unlikely to exist.

Mauna Kea, Hawaii, to search for possible stellar companions. A total of 400 short exposures of 51 Peg were obtained using the facility near-infrared camera outfitted with a set of warm reimaging optics, which converted the plate scale from $0''.15$ to $0''.021 \text{ pixel}^{-1}$ (Matthews et al. 1996). The camera is equipped with a Santa Barbara Research Corporation 256×256 InSb array.

The brightness of 51 Peg is $K = 3.96$ (Campins, Rieke, & Lebofsky 1985) and would saturate the detector if observed with a standard broadband filter. Therefore, we chose to observe with a narrow filter ($\Delta\lambda = 0.053 \mu\text{m}$) centered at $2.26 \mu\text{m}$. The primary mirror of the Keck telescope consists of an array of 36 hexagonal segments each with an edge length of 0.9 m. Hence the longest dimension of the primary mirror corresponds to a baseline of $7 \times 3^{1/2} \times 0.9 = 10.9$ m. Thus $\lambda/D = 0''.043$, and the diffraction pattern of the telescope is fully sampled.

Observations consist of interlaced observations of 51 Peg and two calibrators which are nearby on the sky and have comparable brightness at $2 \mu\text{m}$: τ Peg (HR 8880, HD 220061, A5 V: $K = 4.60$) and HD 218396 (HR 8799, A5 V: $K = 6.18$). Both calibrators are unresolved by optical speckle on the Kitt Peak 4 m telescope (Hartkopf & McAlister 1984). The integration time used to record speckles is 109 ms, and each observation consists of a set of 100 frames. These images were analyzed using classical speckle and bispectral analysis (Labeyrie 1970; Lohmann, Weigelt, & Wirtz 1983) and also using shift-and-add (Christou 1991) techniques to produce diffraction-limited images ($\theta \sim 0''.05$) of 51 Peg.

Figure 6 shows the upper limits for luminous companions to 51 Peg based on the IR Keck observations. The figure shows the 3σ upper limits from speckle reduction and shift-and-add analysis. Speckle analysis gives the best results for small separations, while the shift-and-add technique is more sensitive at large separations from 51 Peg. The diffraction-limited core of the images determines the sensitivity to companions at small separations ($\theta < 0''.05$), speckle noise and scattered light limit sensitivity at intermediate separation ($0''.05 < \theta < 1''.5$), and detector read noise is the limiting factor at large separations ($\theta > 1''.5$).

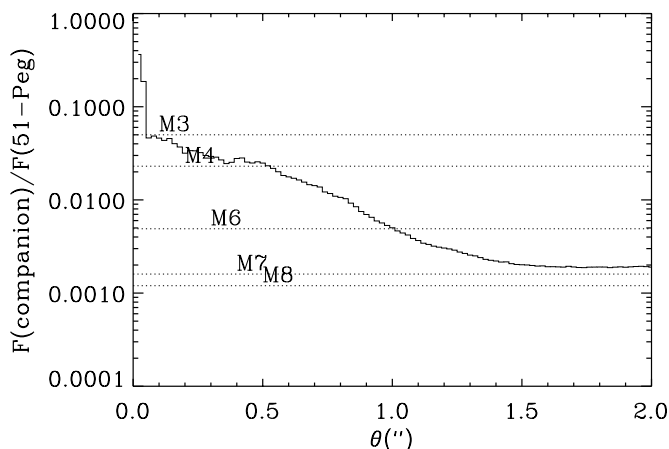


FIG. 6.—Detectability of stellar companions to 51 Peg from IR speckle observations. No companion was found. The solid curve shows detectability limits in terms of the ratio of K-band brightness of any companion relative to that of 51 Peg itself. Horizontal dashed lines labeled by spectral type show the brightness ratio expected for each type. Dwarf companions early than M3 would have been seen from $0''.1$ to $2''.0$ and are ruled out.

Also plotted in Figure 6 are the flux ratios for main-sequence M stars from Leggett (1992). This comparison shows that, except for very close companions (less than $0''.05$), dwarfs having spectral type earlier than M3 are excluded around 51 Peg. The limit improves with increasing distance from the primary, so that at $\theta = 1''.5$, stars earlier than M7 can be ruled out.

Dark companions to 51 Peg might include white or brown dwarfs, both having luminosities that depend on their age. Since 51 Peg and any brown dwarf companion presumably formed at the same time, they have the same age of about 8 Gyr. The luminosity of an 8 Gyr, $80 M_J$ brown dwarf is about $10^{-5} L_\odot$ (Burrows & Liebert 1993) and is therefore well below our detection threshold. Limits on brown dwarf companions must await the long-term radial velocities or astrometry. Constraints on white dwarf companions are more problematic because the age of the white dwarf is unknown. A companion with mass of about $2 M_\odot$ would just have completed its evolution. Assuming our limit is $L_{\text{comp}}/L_{51 \text{ Peg}} = 10^{-3}$ and a white dwarf radius of $R = 0.01 R_\odot$, then the white dwarf surface temperature must exceed 33,000 K to be detectable.

6. TIDAL EFFECTS

The discovery of closely orbiting massive planets raises many interesting questions about tidal effects, such as synchronization and circularization. We have the advantage that much observational and theoretical work has been carried out for the case of companions that are stellar, especially for those which are fully convective (see Verbunt & Phinney 1995 for a recent review). We emphasize here where tidal effects might give rise to observable phenomena and point out that the newly discovered planet around τ Boo might be massive and close enough to force the outer convective envelope of the stellar companion to rotate synchronously with the orbit. These systems may also offer an opportunity to learn more about tidal dissipation in planetary interiors. Some of these issues were also addressed by Rasio et al. (1996).

We assume that 51 Peg is a G2–3 V main-sequence star of age ~ 8 Gyr. The companion is in a circular orbit ($e < 0.01$) at a distance $a = 0.051$ AU and has a mass $m = 0.45 M_J/\sin i$. The likely mass and radius (if similar to Jupiter in composition) are $0.5\text{--}1.0 M_J$ and $R_p \approx 1.3 R_J$ (Guillot et al. 1996). A gas giant at these distances is stable against both Jeans evaporation and photodissociation loss due to extreme-ultraviolet and X-rays from the star (Lin et al. 1996; Guillot et al. 1996).

6.1. Dissipation in the Star

Tidal dissipation within the star circularizes the orbit and synchronizes the stellar rotation to the orbital period. Nearly all of the dissipation occurs in the convective envelope for stars of $M \approx M_\odot$ (Zahn 1977). The convective envelope of mass M_{CE} thus receives all of the tidal torque. It is not understood how the angular momentum eventually gets distributed to the whole star (Scharlemann 1981, 1982; Zahn 1989).

We consider the planet to be a point mass m orbiting the star (mass M and radius R) at a distance a . The time to synchronize the *whole* star is set by the tidal torque and the stellar moment of inertia, I . For weak friction the torque depends on the small tidal lag angle $\alpha \approx (R^3/GM)\omega/t_f$, where ω is the tidal forcing frequency, $t_f \approx (MR^2/L)^{1/3}$ is

the frictional dissipation time (Zahn 1977, 1989, 1994) and L is the stellar luminosity. The resulting synchronization time for the whole star is then

$$t_{\text{synch}}(\text{star}) = \frac{t_f}{6\lambda_2} \frac{I}{MR^2} \left(\frac{M}{m}\right)^2 \left(\frac{a}{R}\right)^6, \quad (1)$$

where λ_2 is close to the apsidal constant (k) when the star is fully convective and is smaller when there is a finite convective zone (Scharlemann 1982; Zahn 1989). In addition, both I/MR^2 and λ_2 are sensitive to the density profile in the star and thus the age. Zahn (1994) tabulated I , t_f , and λ_2 for the zero-age main sequence and found $I/\lambda_2 MR^2 \approx 18$ for $M = M_\odot$ and 24 for $M = 1.1 M_\odot$. For both of these masses, the frictional time is $t_f = 0.44$ yr, so we just take values for $M = M_\odot$, in which case we get

$$t_{\text{synch}}(\text{star}) = 1.2 \left(\frac{M}{m}\right)^2 \left(\frac{a}{R}\right)^6 \text{ yr}. \quad (2)$$

For the case of 51 Peg this yields

$$t_{\text{synch}}(51 \text{ Peg}) \approx 10^{13} \sin^2 i \left(\frac{R_\odot}{R}\right)^6 \left(\frac{M}{M_\odot}\right)^{8/3} \text{ yr}, \quad (3)$$

much too long for any appreciable effects and consistent with the slow measured stellar rotation. Rasio et al. (1996) came to a similar conclusion. In addition, we note that the observed slow stellar rotation ($P = 30\text{--}37$ days) implies that the companion mass cannot be very large. For example, if $\sin i < 2.8 \times 10^{-2}$, i.e., $m > 15 M_J$, then the synchronization time becomes comparable to the age of the star, and we would expect the star to be synchronously rotating, which is not the case. Thus the slow rotation of the star in the 51 Peg system implies that the companion mass is less than $15 M_J$. Similar limits on companion mass stem from the low X-ray flux from 51 Peg, which shows that it was not tidally spun up (Pravdo et al. 1996).

However, as we noted earlier, all of this torque is exerted only on the convective zone, and it might be the case that the transferred angular momentum merely resides there. For solar mass stars where $M_{\text{CE}} \sim 0.01\text{--}0.1 M_\odot$, this can reduce the observed (surface) synchronization timescales by about an order of magnitude. This consideration, if better developed, might permit more stringent upper limits to be placed on the companion mass.

For the recently detected companion to τ Boo ($P_{\text{orb}} = 3.31$ days and $K = 468 \text{ m s}^{-1}$; Butler et al. 1997), tidal considerations may be important because of the greater mass of the companion ($m \sin i = 3.8 M_J$). This system gives $t_{\text{synch}}(\tau \text{ Boo}) \approx 7.5 \times 10^{10} \sin^2 i \text{ yr}$ for solar parameters and for spinning up the whole star. In this case, a convective envelope of $M_{\text{CE}} \approx 10^{-2} M_\odot$ could easily be synchronized in less than the age of the system. This amount of angular momentum transport is not susceptible to the secular instabilities discussed by Rasio et al. (1996). Indeed, the inferred mass for the planet around τ Boo is larger than the minimum needed for stability (Rasio et al. 1996):

$$\frac{m}{M_J} > 2.16 \left(\frac{M}{M_\odot}\right)^{1/3} \left(\frac{R}{R_\odot}\right)^2 \left(\frac{4 \text{ days}}{P_{\text{orb}}}\right)^{4/3}, \quad (4)$$

where we have set $I = 0.07MR^2$. Hence the whole star can be brought into synchronicity without reaching a tidal instability.

Since older stars with convective zones will have spun down to periods longer than a few days within a few billion years, the detection of anomalous rapid rotation can be viewed as an additional indicator of the planet's existence. It is the extent of the convective zone in the star that determines this spin-down time, and for stars near M_\odot the mass of the convective envelope is a very sensitive function of the mass and evolutionary state. Further theoretical work on the way in which this dissipation comes about is needed, especially if τ Boo (or other systems) are found to harbor anomalously rapid rotators. Indeed, one might want to consider rapid rotation as a secondary indicator for the presence of close companions.

The tight agreement in both the timescale for synchronization and the mass needed for stable dynamics in τ Boo might just be a coincidence, or it might be related to the concept that synchronization of other planets has pulled them into the star. In this case, one might consider a search for close massive planets around stars with radiative zones on the main sequence. In this case, the tidal dissipation for tight orbits would be negligible and massive planets might survive at close radii. The only way for these types of stars to become synchronized is during the main-sequence contraction phase.

As another effect, the orbit might also be circularized by the tidal dissipation in the convective zone of the star. The timescale for this to occur is $t_{\text{circ}} \approx t_f (M^2/mM_{\text{CE}})(a/R)^8$, which is always much longer than a Hubble time for the present parameters of 51 Peg. We thus agree with Rasio et al. (1996) that the circular orbit could not have been tidally induced during the main-sequence lifetime of the star. It might be that the circularization occurred sometime during the final contraction of the star onto the main sequence, when it both was larger and had a bigger convective zone. Indeed, circularization during Hayashi contraction seems to be the best explanation for the observed period of 5–8 days at which orbits are mostly circular in late-type binaries (Zahn & Bouchet 1989). Another alternative, which we discuss next, is that dissipation in the planet circularized the orbit.

In the context of the present tidal theory, our timescales should be viewed as rather secure lower limits. This is because we have used the full eddy viscosity, even though the eddy turnover time is typically longer than the orbital period. Many have argued that the viscosity is much smaller (and t_f much longer) in this case (Goldreich & Nicholson 1977; see Zahn 1989 for a full discussion). Zahn & Bouchet (1989) showed, however, that much longer dissipation times would be at odds with the observed period-eccentricity relation described above.

6.2. Dissipation in the Planet

Another issue to address is the rate of tidal dissipation within the planet. This is even more uncertain than the above discussion, as we only have a lower limit to the planetary mass, no direct information on its radius R_p , and only inferences on the dissipation mechanism itself. Most models for Jupiter-mass objects (where Coulomb effects are important) can be roughly represented as $n = 1$ polytropes (Hubbard 1974) which have $I_p/k_p m R_p^2 \approx 1$ (Mozt 1952). Objects much more massive than Jupiter are better modeled as $n = 3/2$ polytropes, with $I_p/k_p m R_p^2 = 1.4$. In order to be able to relate our results to prior inferences from Jupiter and other gas giants, we write the synchronization

time in terms of the tidal quality factor Q defined by Goldreich & Soter (1966) and use the moment of inertia/apsidal constants from above (which really do not matter for this case) to obtain

$$t_{\text{synch}}(\text{planet}) \approx Q \omega_d \frac{m}{M} \left(\frac{a^3}{GM} \right) \left(\frac{a}{R_p} \right)^3, \quad (5)$$

where $\omega_d = 2\pi/P_d$ is the difference in frequency between corotation and the initial value. For 51 Peg we find $t_{\text{synch}} \approx Q(R_p/R_p)^3/\sin i$ yr when $P_d = P_{\text{orb}}$. Goldreich & Soter (1966) found the circularization time as

$$t_{\text{circ}} \approx \frac{4Q}{63} \frac{m}{M} \frac{P_{\text{orb}}}{2\pi} \left(\frac{a}{R_p} \right)^5. \quad (6)$$

Hence, internal dissipation in the planet will only circularize the orbit in 5 Gyr if $Q < 8 \times 10^5 \sin i (R_p/R_p)^5$ for 51 Peg and $Q < 2.5 \times 10^6 \sin i (R_p/R_p)^5$ for τ Boo. Much less stringent limits are applicable if one wants to demand synchronous rotation of the planet (i.e., the planet always shows the same face to the star).

For solid planets, the tidal Q 's are in the range 100–1000, and so there would be no problem with either circularization or synchronization of a solid planet in 51 Peg. The situation is different for a gaseous/liquid planet, where we can relate Q to the frictional time defined earlier $Q \sim t_f(Gm/R_p^3)/\omega_{\text{orb}}$. One would presume that t_f is the more fundamental physical parameter, in which case Q 's obtained in one binary can be related to those obtained in another only after disentangling the other important timescales (basically the planet's dynamical time and the perturbing frequency). Luckily, these timescales are basically the same when we compare 51 Peg B to Jupiter, since the limits of Q for Jupiter are obtained from the behavior of its satellites, which orbit with comparable orbital periods (days).

The inferred Q for Jupiter is $Q_J > 10^5$, so as to avoid excessive orbital evolution of its satellites (Goldreich & Soter 1966). In addition, if tidal torques are responsible for the development of the orbital resonances of the satellites, then $Q_J < 10^6$ (Goldreich & Soter 1966; Yoder 1979; Yoder & Peale 1981; see Malhotra 1991 for a recent critical discussion). Since all current theories of the structure for Jupiter find a nearly fully convective object (Guillot et al. 1994), it is natural to first ask whether a turbulent viscosity can explain Q_J . Hubbard (1974) first estimated this and found $Q_J \sim 5 \times 10^6$. Goldreich & Nicholson (1977) later argued that the eddy viscosity must be reduced when the eddy turnover time is longer than the forcing frequency and concluded that Q_J (eddy viscosity) $\approx 5 \times 10^{13}$ (this is the same issue alluded to earlier in the context of the eddy viscosity in the convective zone of the star). One of the more recent detailed efforts on alternative sources of viscosity is that of Stevenson (1983), who found that $Q_J \approx 4 \times 10^4$ for some fraction of its life. This highlights how little is understood about the origin of the value of Q for Jupiter, much less for these newly discovered and potentially very different planets.

We are thus reluctant to say that the 51 Peg planet is in a circular orbit due to internal dissipation in either the star or the planet. It is likely that there is enough internal dissipation for it to be synchronously rotating and thus always showing the same face to the star. There is probably hope

that a slightly eccentric short orbital period system will be found that allows for a lower limit on Q . In the absence of that information, we cannot determine with certainty whether the circular orbits in either 51 Peg or τ Boo are due to internal dissipation in the planet or were primordial.

7. DISCUSSION

The Doppler velocity variations of 51 Peg, along with all of the photometric and spectroscopic observations for it, are consistent with a planetary object in circular orbit at 0.051 AU. These results are in complete agreement with those of Mayor & Queloz (1995). Recently, additional confirmation of the 51 Peg Doppler periodicity has come from the AFOE group (Noyes et al. 1995; Kennelly et al. 1995). No other explanation besides an orbiting companion appears viable at present. For likely orbital inclinations of 30° – 90° , the mass of the companion is 0.45 – $0.90 M_J$. Ninety percent of randomly oriented orbital planes will lie within this range of inclination. The age of 51 Peg is estimated to be at least 5×10^9 Gyr (Edvardsson et al. 1993), and during that time the planet may have suffered some tidal evolution if the planet's dissipation Q -value is smaller than $\sim 10^6$, as may be the case for Jupiter. Otherwise, the circular orbit may be primordial.

Still uncertain is the formation history of this planet. Its extremely small orbital radius challenges theories of gas-giant planet formation that unanimously predict formation distances of several AU (Lissauer 1995; Boss 1995). It remains unknown where the planet formed and how it arrived at its current location. Lin et al. (1996) propose protoplanetary migration, halted by the rotational tidal torques or the disk gap near the surface of the protostellar 51 Peg. The present observations rule out additional planetary companions having $m \sin i > 0.3 M_J$ within 1 AU, and rule out companions having $m \sin i > 1 M_J$ within 2 AU (Fig. 5). This absence of additional Jupiter-mass companions suggests that the inner planet at 0.05 AU arrived there without the benefit of dynamical shepherding from neighboring planets. Nor is there evidence of Jupiter-sized planets that might have gravitationally scattered the inner planet into its present location. While giant planets farther than 2 AU cannot be ruled out, a star is unlikely to capture a planet that was scattered inward from such great distances (Rasio & Ford 1996). The common occurrence of 51 Peg-like planets (Butler et al. 1997) points toward a formation mechanism that results almost deterministically, not serendipitously, from initial conditions.

The grid of model planets at very small orbital radii by Guillot et al. (1996) and Burrows et al. (1996) gives predicted radii and luminosities of planets with a variety of separations, masses, and chemical compositions. They show that a $1 M_J$ planet at 0.05 AU is stable against a variety of potential nemeses and will have an effective temperature of 1250 K and a radius of $1.2 R_J$. A rocky planet of the same mass would have a radius of $0.3 R_J$. In principle, one could spectroscopically distinguish planets made of H-He from those made of rock. But the small angular separation ($0''.003$) from the star inhibits the acquisition of a spectrum of the planet. However, multiple spectra (hundreds) of the primary star, 51 Peg, may permit extraction of the faint (10^{-4} as bright) spectrum of the planetary companion (R. Noyes 1996, private communication; D. Finkbeiner 1996, private communication). The IR contribution from the planet would be 3 orders of magnitude less than that of the star.

Spectroscopic searches for the weak, superimposed IR spectrum of the planet may be possible.

Not surprisingly, the first few planets that have been detected have masses similar to or larger than Jupiter. The reflex velocity varies linearly with companion mass and inversely as the square root of orbital radius, implying that the detections around 51 Peg, 70 Vir, 47 UMa, and HD 114762 share a selection bias of high mass and of orbital proximity, as well as a bias toward edge-on orbital planes that increase the Doppler signal. Our more recent discoveries of planetary companions to HR 3522 (G8 V), HR 5185 (F7 V), and HR 458 (F8 V) all exhibit orbital periods of less than 15 days and values of $m \sin i$ less than $4 M_J$ (Butler et al. 1997; Baliunas et al. 1997). These stars may be systematically metal-rich, having $[\text{Fe}/\text{H}] = +0.1$ to $+0.3$ (Chavez, Malagnini, & Morossi 1995; Taylor 1996), reminiscent of the high metallicity of 51 Peg. Perhaps high metallicity promotes the “51 Peg phenomenon” of short-period, circular planetary companions. Alternatively, perhaps the presence of close planetary companions indicates contamination of the photosphere by the previous infall of metal-rich planets (D. N. C. Lin 1996, private communication). Any correlation of metallicity with planetary characteristics would certainly provide a valuable constraint on models of formation.

At the time of writing, six companions having $m \sin i < 7 M_J$ have been found by the two surveys of Mayor and Queloz and ourselves which operate at high Doppler precision of $\sim 10 \text{ m s}^{-1}$. The companions orbit the stars 51 Peg, HR 3522 (55 Cnc), HR 5185 (τ Boo), HR 458 (ν And), HR 4277 (47 UMa), and HR 5072 (70 Vir). These two high-precision surveys are sensitive to masses in two nominal ranges, $m < 15 M_J$ and $10 M_J < m < 70 M_J$ (prematurely named “planets” and “brown dwarfs,” respectively). The surveys thus permit an assessment of the relative numbers of companions in each mass category within 5 AU. Interestingly, all six companions found to date fall in the category of lower mass, $m \sin i < 10 M_J$, despite the smaller mass range. The two surveys have not found any companions having $m \sin i$ between 10 and $70 M_J$, despite their ease of detection. No selection effect in our sample avoided brown dwarf companions. Therefore, the occurrence rate of brown dwarf companions within 5 AU (0 out of 120 in our survey) is clearly less than a few percent.

Indeed, Mayor et al. (1997) have reported that eight out of 570 GK dwarfs revealed velocity variations that give $m \sin i < 40 M_J$, thus implying a frequency of occurrence of 1.4%. Including higher mass companions up to $75 M_J$, we estimate that $3\% \pm 1\%$ of all GK dwarfs have a companion with mass between 10 and $75 M_J$ orbiting within 5 AU. This implies an average mass function, per star, of

$$\frac{dN}{dM} = \frac{0.03}{65} = 0.00046 \text{ BD companions } M_J^{-1}$$

within 5 AU, over the brown dwarf (BD) domain of masses. However, the occurrence of planetary-mass companions per unit mass interval is apparently higher. Within our survey of 120 stars, five low-mass, planetary companions ($m \sin i < 4 M_J$) have been found. This yields a rate of occurrence of 4% per $4 M_J$, or a mass function, per star, of

$$\frac{dN}{dM} = 0.010 \text{ planets } M_J^{-1}.$$

The planetary mass function appears to be 20 times that of the brown dwarfs. This estimate of the planetary mass function will likely increase as lower mass planets become detectable.

Apparently there is a discontinuity in the mass distribution of companions at about $10 M_J$, with more companions having lower mass. Mayor et al. (1992, 1997) and Mazeh et al. (1996) have found clear evidence for the more massive “brown dwarf” companions. These detections demonstrate that the more massive “brown dwarf” companions exist and presumably form within 5 AU. The surveys at high and low Doppler precision are thus marginally mutually consistent with each other: at low precision the brown dwarf candidates exhibit a 3% occurrence, while at high precision we have (unluckily) found no companions having $m \sin i > 10 M_J$ out of only 120 stars. We would have expected to find only about three of them. The occurrence of brown dwarf companions is presumably so low that none have shown up in the small stellar samples observed at high Doppler precision. Duquennoy & Mayor (1991) and Mazeh, Mayor, & Latham (1997) describe the prospects for using orbital eccentricity as the discriminant between the planetary and “brown dwarf” populations of companions. If, as we expect, companions are discovered that have both very low mass and large eccentricity, more sophisticated physical scenarios of formation will be required.

We thank G. Basri, A. Burrows, Doug Finkbeiner, Doug Lin, Michel Mayor, Bob Noyes, Didier Queloz, Fred Rasio, D. Saumon, and D. Werthimer for valuable discussions. H. Hauser and P. Shirts obtained and analyzed some of the spectra. We thank J. Valenti for help with the Doppler analysis and S. S. Vogt for refurbishing the echelle spectrometer, with fine tuning by Tony Misch. We thank Marc Davis and Walter Herrick for use of their Sun Microsystems workstations. We are grateful to D. Soderblom, B. Jones, G. Smith, C. McCarthy, and D. Fischer for donating telescope time from their observing programs to help carry out some of these observations. We thank W. Harrison, without whom the IR speckle observations would not have been made. We acknowledge generous support from NASA (NAGW 3182), NSF (AST 95-20443), and SUN Microsystems. L. B. acknowledges support as an Alfred P. Sloan Foundation fellow. J. R. G. was supported by the Packard Foundation.

REFERENCES

- Baliunas, S. L., Henry, G. W., Donahue, R. A., Fekel, F. C., & Soon, W. H. 1997, *ApJ*, submitted
 Boss, A. P. 1995, *Science*, 267, 360
 Burrows, A., Hubbard, W. B., Lunine, J. I., Guillot, T., Saumon, D., Marley, M., & Freedman, R. S. 1996, in *Proc. Int. Conf. on Sources and Detection of Dark Matter in the Universe*, ed. D. Sanders et al. (Nucl. Phys. B Proc. Suppl.), in press
 Burrows, A., & Liebert, J. 1993, *Rev. Mod. Phys.*, 65, 301
 Burrows, A., Saumon, D., Guillot, T., Hubbard, W. B., & Lunine, J. I. 1995, *Nature*, 375, 299
 Butler, R. P., Bell, R. A., & Hindsley, R. B. 1996a, *ApJ*, 461, 362
 Butler, R. P., & Marcy, G. W. 1996, *ApJ*, 464, L153
 Butler, R. P., Marcy, G. W., Williams, E., Hauser, H., & Shirts, P. 1997, *ApJ*, in press
 Butler, R. P., Marcy, G. W., Williams, E., McCarthy, C., & Vogt, S. S. 1996b, *PASP*, 108, 500
 Campins, H., Rieke, G. H., & Lebofsky, M. J. 1985, *AJ*, 90, 896
 Carroll, J. A. 1928, *MNRAS*, 88, 548
 Chavez, M., Malagnini, M. L., & Morossi, C. 1995, *ApJ*, 440, 210
 Christou, J. C. 1991, *PASP*, 103, 1040

- Cochran, W. D., & Hatzes, A. P. 1994, in *Planetary Systems: Formation, Evolution, and Detection*, ed. B. F. Burke, J. H. Rahe, & E. E. Roettger (Dordrecht: Kluwer), 281
- Duquennoy, A., & Mayor, M. 1991, *A&A*, 248, 485
- Edvardsson, B., Anderson, J., Gustafsson, B., Lambert, D. L., Nissen, P. E., & Tomkin, J. 1993, *A&A*, 275, 101
- François, P., Spite, M., Gillet, D., Gonzalez, J.-F., & Spite, F. 1996, *A&A*, 310, L13
- Goldreich, P., & Nicholson, P. D. 1977, *Icarus*, 30, 301
- Goldreich, P., & Soter, S. 1966, *Icarus*, 5, 375
- Guillot, T., Burrows, A., Hubbard, W. B., Lunine, J. I., & Saumon, D. 1996, *ApJ*, 459, L35
- Guillot, T., Gautier, D., Chabrier, G., & Mosser, B. 1994, *Icarus*, 112, 337
- Guinan, E. 1995, *IAU Circ.* 6261
- Hartkopf, W. I., & McAlister, H. A. 1984, *PASP*, 96, 105
- Hatzes, A. P., Cochran, W. D., & Johns-Krull, C. 1996, *ApJ*, in press
- Henry, G. W., Baliunas, S. L., Donahue, R. A., Soon, W. H., & Saar, S. H. 1996, *ApJ*, 474, 503
- Houk, N. 1995, *IAU Circ.* 6253
- Hubbard, W. B. 1974, *Icarus*, 23, 42
- Kennelly, T., Brown, T., Rowland, C., Horner, S., Korzennik, S., Krockenberger, M., Nisenson, P., & Noyes, R. 1995, *BAAS*, 187, 7005
- Labeyrie, A. 1970, *A&A*, 6, 85
- Latham, D. W., Mazeh, T., Stefanik, R. P., Mayor, M., & Burki, G. 1989, *Nature*, 339, 38
- Leggett, S. L. 1992, *ApJS*, 82, 351
- Lin, D. N. C., Bodenheimer, P., & Richardson, D. C. 1996, *Nature*, 380, 606
- Lissauer, J. J. 1995, *Icarus*, 114, 217
- Lohmann, A. W., Weigelt, G. P., & Wirtzner, B. 1983, *Appl. Opt.*, 22, 4028
- Malhotra, R. 1991, *Icarus*, 94, 399
- Marcy, G. W., & Butler, R. P. 1996, *ApJ*, 464, L147
- Matthews, K., Ghez, A. M., Weinberger, A. J., & Neugebauer, G. 1996, *PASP*, 108, 615
- Mayor, M., Duquennoy, A., Halbwachs, J.-L., & Mermilliod, J.-C. 1992, in *IAU Colloq. 135, Complementary Approaches to Double and Multiple Star Research*, ed. H. McAlister & W. Hartkopf (ASP Conf. Ser., Vol. 32; San Francisco: ASP), 73
- Mayor, M., & Queloz, D. 1995, *Nature*, 378, 355
- Mayor, M., Queloz, D., Udry, S., & Halbwachs, J. L. 1997, in *IAU Colloq. 161, Astronomical and Biochemical Origins and Search for Life in the Universe*, ed. C. Cosmovici, S. Bowyer, & D. Werthimer, 313
- Mazeh, T., Latham, D. W., & Stefanik, R. P. 1996, *ApJ*, 466, 415
- Mazeh, T., Mayor, M., & Latham, D. W. 1997, *ApJ*, submitted
- Motz, L. 1952, *ApJ*, 115, 562
- Nakajima, T., Oppenheimer, B., Kulkarni, S. R., Matthews, D. G., & Durran, S. 1995, *Nature*, 378, 463
- Noyes, R. W., Hartmann, L., Baliunas, S. L., Duncan, D. K., & Vaughan, A. H. 1984, *ApJ*, 279, 763
- Noyes, R., Korzennik, S., Krockenberger, M., Nisenson, P., Brown, T., Kennelly, T., & Rowland, C. 1995, *IAU Circ.* 6251
- Perryman, M. A. C., et al. 1996, *A&A*, 310, L21
- Pettersen, B. R., Hawley, S. L., & Fisher, G. H. 1992, *Sol. Phys.*, 142, 197
- Pravdo, S. H., Angelini, L., Drake, S. A., Stern, R. A., White, N. E. 1996, *New Astron.*, 1, 171
- Rasio, F. A., & Ford, 1996, *Science*, 274, 954
- Rasio, F. A., Tout, C. A., Lubow, S. H., & Livio, M. 1996, *ApJ*, 470, 1187
- Saumont, D., Hubbard, W. B., Burrows, A., Guillot, T., Lunine, J. I., & Chabrier, G. 1996, *ApJ*, 460, 993
- Scharlemann, E. T. 1981, *ApJ*, 246, 292
- . 1982, *ApJ*, 253, 298
- Soderblom, D. R. 1983, *ApJS*, 53, 1
- Stevenson, D. J. 1983, *J. Geophys. Res.*, 88, 2445
- Taylor, B. J. 1996, *ApJS*, 102, 105
- Valenti, J. A., Butler, R. P., & Marcy, G. W. 1995, *PASP*, 107, 966
- Verbunt, F., & Phinney, E. S. 1995, *A&A*, 296, 709
- Vogt, S. S. 1987, *PASP*, 99, 1214
- Yoder, C. F. 1979, *Nature*, 279, 767
- Yoder, C. F., & Peale, S. J. 1981, *Icarus*, 47, 1
- Zahn, J. P. 1977, *A&A*, 57, 383
- . 1989, *A&A*, 220, 112
- . 1994, *A&A*, 288, 829
- Zahn, J. P., & Bouchet, L. 1989, *A&A*, 223, 112